Colloid Polym Sci 274:356–367 (1996)

ORIGINAL CONTRIBUTION

J.V. Mitrancheva
C.D. Dushkin
P. Joos

Kinetics of the surface tension of micellar solutions: Comparison of different experimental techniques

Received: 8 May 1995
Accepted: 3 September 1995

J.V. Mitrancheva · Dr. C.D. Dushkin (✉)
Laboratory of Thermodynamics and
Physico-chemical Hydrodynamics
Faulty of Chemistry
University of Sofia
1 James Baucher Blvd.
1126 Sofia, Bulgaria

P. Joos
Laboratory of Dynamic Surface Tension
Department Scheikunde
Antwerp University
1 Universiteitsplein
2610 Wilrijk, Belgium

Abstract The kinetics of the surface tension of micellar solutions of nonionic surfactant Triton X-100 is measured experimentally by means of three different techniques: oscillating jet, maximum bubble pressure and inclined plate. They allow to study the micellization kinetics at various time scales (from a few milliseconds to a few seconds) in fairly large concentration region up to 50 times CMC. The experimental data are satisfactorily explained by a theoretical model accounting for the kinetics of micellization, diffusion of surfactant species and expansion of the bubble interface. By this model are computed the characteristic times of diffusion and micellization, which are of comparable magnitude (about 5 to 200 ms), and the Gibbs' elasticity. The micellization time constant corresponds to the slow relaxation process known to coincide with the disintegration of micelles. Comparing our data with other data from literature one can conclude that more realistic information for the micellization kinetics is obtained by the maximum bubble pressure and the oscillating jet method. The inclined plate seems too slow to measure the relaxation processes in micellar solutions of this surfactant.

Key words Micellization kinetics – maximum bubble pressure – oscillating jet – inclined plate – Triton X-100 – Gibbs' elasticity

Introduction

The micellar surfactant solutions play an important role in many practical processes where the surface properties of the solutions are determined by the amount of adsorbed substance which changes with time. The adsorption kinetics is influenced by the micelles present in the solution at surfactant concentrations exceeding the critical micelle concentration (CMC). Being aggregates of surfactant monomers, the micelles act as additional sources of material which can appreciably affect the surface tension relaxation.

Since, for a number of surfactants, the relaxation of the micelles is a very fast process, it is difficult to account for its effect on the surface properties of the solutions [1–3]. Also the micelles are polydisperse species contributing in a complicated way to the surfactant diffusion and adsorption which is laborious for theoretical interpretation [4]. That is why one surface experimental method is not enough to obtain data consistent with the micellization kinetics as revealed by the chemical relaxation techniques [5–7]. Usually the characteristic time of micellization (or the demicellization rate constant) is extracted from the experimental data for the surface tension kinetics by approximate theoretical models [1, 2, 8, 9]. Due to the simplifications these models exaggerate the contribution of a part of the experimental data collected at times much shorter (or longer) than the characteristic time of diffusion (or of micellization). This leads to micellization time

constants which can differ by several times depending on the experimental method and/or on the used theoretical model.

Our aim here is to study the kinetics of micellization by using complementary surface relaxation methods and processing of the data by more sophisticated theoretical model. For this purpose we apply three classical surface methods: oscillating jet, inclined plate and maximum bubble pressure. By these methods we detect the surface tension at different time scales which allow to compare the experimental results as well as to make more definite conclusions from the model parameters. The theoretical model is based on solving the respective diffusion equations assuming the micellization kinetics as a pseudo-first-order chemical reaction [1, 3]. This model reflects as much features of the experimental system as possible to obtain analytical solution. For example, the experimental data from the maximum bubble pressure method are fitted by an equation for the dynamic surface tension accounting also for the rate of bubble expansion. As model surfactant we chose Triton X-100 whose micellization kinetics is extensively studied by both surface [1, 2, 8, 10, 11] and bulk relaxation methods [12, 13].

Experimental methods

The experiments were performed with aqueous solutions of nonionic surfactant Triton X-100 (Serva) at 10 different concentrations ranging between $1 \times$ CMC and $50 \times$ CMC, where CMC $= 1.55 \times 10^{-7}$ mol/cm^3. The experiments were carried out at room temperature 22°–25 °C.

Oscillating jet method

Detailed description of the method is given by Defay and Petre [14]. The liquid jet emerges under constant pressure from a slightly elliptical capillary where a new surface is created. The liquid flows from the region of higher pressure (maximum curvature) to the region of lower pressure (minimum curvature) to give stationary standing waves. Due to gravity the horizontal jet is in fact of parabolic shape. When the flowing liquid is a surfactant solution, the surfce tension at the jet/air interface decreases with increasing the distance from the orifice due to surfactant adsorption. The surface tension gradient tends to cause a flow on the surface toward the orifice which, together with the viscous drag on the underlying liquid, reduces the mean velocity of the jet. The lowering of the surface tension along the jet generates in turn a pressure gradient, tending to accelerate the jet [15].

The liquid jet illuminated by parallel beam of light acts as a sort of cylindrical lens focusing the light at different focal lines onto a screen corresponding to different parts (oscillations) from the jet. The longer the length of one oscillation, the further the focal line. The distance between two focal lines, measured by a traveling long-focus microscope, gives the length of the stationary wave. With increasing the surfactant concentration the surface tension decreases resulting in elongation of the oscillations. Such elongation was observed in our experiments with Triton X-100 at concentrations above 10 times CMC.

To calculate the surface tension from the jet profile one has to resolve the hydrodynamics problem for the liquid flow inside the jet. Considering three dimensional viscous flow one can obtain for the surface tension [14, 16–18]

$$\sigma = \frac{4\rho Q^2}{6r\lambda^2}\left[\frac{1+(37q^2/24r^2)}{1+(5\pi^2r^2/3\lambda^2)}\right] \times\left[1+2\left(\frac{\mu\lambda}{\rho Q}\right)^{\frac{3}{2}}+3\left(\frac{\mu\lambda}{\rho Q}\right)^2\right], \tag{2.1}$$

where Q is the flow rate, r is the mean radius of the capillary, λ is the length of one oscillation (considered also as a wavelength), μ and ρ are respectively the viscosity and the density of liquid, q is the amplitude of the jet oscillation. We calculated the surface tension by the following approximate equation:

$$\sigma = \frac{4\rho Q^2}{6r\lambda^2}\left[\frac{1}{1+(5\pi^2r^2/3\lambda^2)}\right], \tag{2.2}$$

since in our experiment

$$q \ll r\sqrt{\frac{24}{37}}, \tag{2.3}$$

and $\mu\lambda/\rho Q \ll 1$ (cf. Eq. (2.1)).

According to the procedure described in refs. [17, 19] the surface age t is obtained from the expression

$$t = \frac{x}{v_s}, \tag{2.4}$$

where the surface velocity v_s is defined as

$$v_s = \frac{Q}{\pi r^2}, \tag{2.5}$$

and the distance x is measured from the first wavelength λ, taken as reference line during all the experiments.

Three elliptical capillaries of different mean radii were used: $r_1 = 0.0342$ cm; $r_2 = 0.0288$ cm and $r_3 = 0.0218$ cm. The flow rate Q of the jet was determined after each experiment by measuring the amount of solution flowing into a standard vessel for certain time. At constant pressure the flow rates depend on the capillary radius and are

about 1.45 ml/s for capillary 1, 0.99 ml/s for capillary 2 and 0.62 ml/s for capillary 3. They produce jet waves of different number and length λ. For capillary 1 λ varies between 0.711 cm (second wave) and 0.741 cm (eleventh wave) at concentration $1 \times$ CMC. For low surfactant concentrations the first wave at the jet orifice is appreciably longer than the next ones which leads, in view of Eq. (2.2), to lower calculated surface tension. That is why we disregard this wave. With increasing of the surfactant concentration the length of the waves increases whereas their number decreases. At the highest concentration $50 \times$ CMC the values of λ are 0.919 cm (first wave) and 1.095 cm (fifth wave). After the last wave the jet disperses. Each measurement of λ was carried out twice in order to obtain reproducible results.

Figure 1 represents typical results for the surface tension measured by the three capillaries at surfactant concentration $15 \times$ CMC. It is seen that the data points obtained by capillaries 2 and 3 practically coincide, whereas the surface tension measured by capillary 1 is always higher. Since at smaller capillary radius r the wave amplitude q should be larger, the condition (2.3) can be no longer valid. Subsequently, neglecting the respective term in Eq. (2.2) leads to lower values for σ with capillaries 2 and 3 than with capillary 1. The same feature is demonstrated also at lower surfactant concentrations where the difference in σ can be even larger. At higher surfactant concentrations, however, this difference becomes negligible because q decreases (the wavelengths λ increase) which makes the condition (2.3) of better validity.

The time scale of the oscillating jet method is typically between one millisecond and several hundredths of a second. By decreasing the capillary radius it is possible to access very short ages t of the liquid jet. For example, with capillary 1 were measured initial times $t \approx 2$ ms, while with capillary 3 – $t \approx 0.9$ ms. However, the surface tension calculated from the first few waves corresponding to very short times $t < 3$ ms is too high and must be disregarded. Even for pure water the right surface tension has been found after the fourth wave [1]. This phenomenon is very tangible at surfactant concentrations up to several times CMC. The values of σ larger than the surface tension of pure water (72.5 dyn/cm) in Fig. 1 are due to a shortcoming of Eq. (2.1) derived originally for plug flow in the jet. This is not the case along the first few waves close to the orifice where transition from Poiseulle flow in the capillary to plug flow in the jet occurs. To avoid this problem the data points larger than 72.5 dyn/cm are not considered in computing the surface tension by the theory (see below).

Fig. 1 Time dependence of the surface tension of micellar solution of Triton X-100 ($15 \times$ CMC) measured by the oscillating jet method. Empty and full figures correspond to two successive measurements by the respective capillary

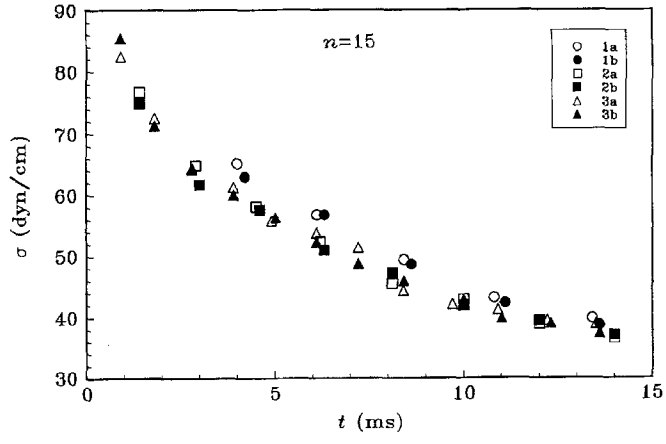

Inclined plate method

The used experimental setup is that described by Van den Bogaert and Joos [20] (see also ref. [21]). The surfactant solution was allowed to flow over an inclined glass plate with an angle of inclination $\alpha = 4°$ kept constant throughout the experiments. The plate length is about 2 m. Two other small glass plates of the same length are fixed at the side edges to form a canal of width $B = 2$ cm. At the inlet (top of the canal) a fresh air/water surface is formed; with increasing the distance x from the inlet surfactant molecules adsorb onto this surface. Due to the different amount of adsorbed surfactant molecules with time the surface tension decreases with increasing the distance x from the inlet. The surface tension is measured as a function of x by using a Wilhelmy plate connected to the side arm of Statham force transducer.

The surface age t at some distance x from the inlet is calculated by Eq. (2.4) although there are effects that can complicate this procedure [17, 19, 20, 22]. The surface velocity v_s is given by the equation [20]:

$$v_s = \frac{\rho g h^2 \sin \alpha}{2\mu}, \tag{2.6}$$

where g is the gravity acceleration and h is the thickness of the flowing layer

$$h = \left(\frac{3\mu Q}{B\rho g \sin \alpha} \right)^{1/3}. \tag{2.7}$$

The flow rates Q were between 6.3 and 7.0 ml/s providing liquid layer of thickness about 1 mm.

Typical results for the surface tension are plotted in Fig. 2, implying that in this method the surface age t can range from tenths of a second to few seconds.

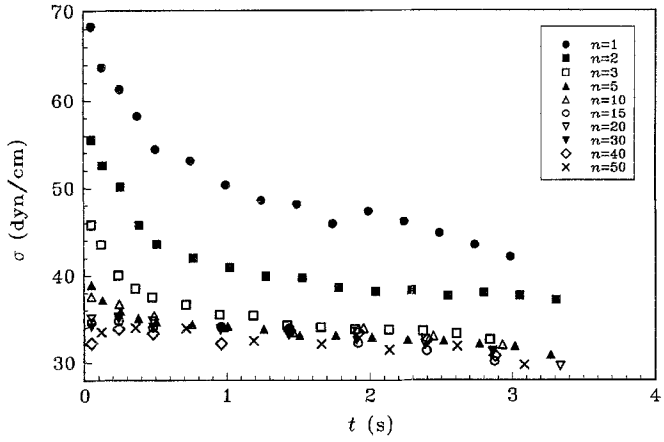

Fig. 2 Surface tension of micellar Triton X-100 solutions measured by the inclined plate method. The surfactant concentration n is represented in times CMC

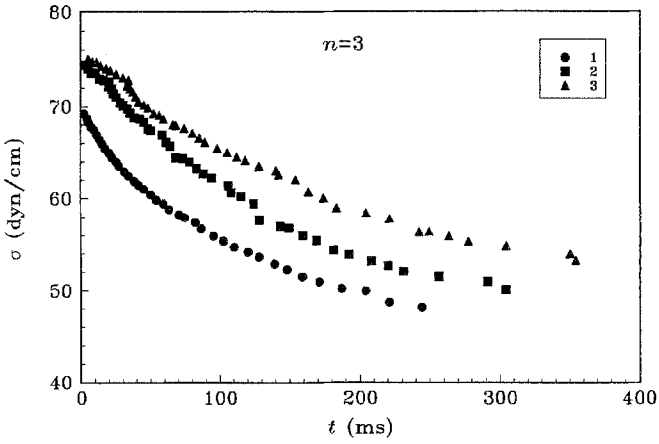

Fig. 3 Effect of exhausting of surfactant on the dynamic surface tension measured by the maximum bubble pressure method (Triton X-100 concentration 3 × CMC). The numbers show the number of successive measurement

Maximum bubble pressure method

Here we used the apparatus described in refs. [10, 11] which is applicable to very short life-times (high bubbling frequencies). The pressure inside the system is measured by a pressure transducer. This pressure is equal to the maximum bubble pressure because the system is of volume much larger than the volume of the bubble itself. The frequency of bubble formation ν is measured by an acoustic system with a microphone. The signals from different detectors are processed by computer which calculates the dynamic surface tension as a function of time corrected for dead time τ_{dead}

$$\tau_{dead} = \frac{Q}{\nu k p}\left(1 + \frac{3r}{2R}\right). \tag{2.8}$$

Here $p = 2\sigma/R$, R is the actual bubble radius at the moment of measurement of the pressure,

$$k = \frac{\pi r^4}{L\mu_g}$$

is a constant calculated assuming Poiseulle flow of the gas along the capillary of length L, μ_g is the gas viscosity. The dead time is determined from the change in the slope of the curve pressure vs gas flow rate Q corresponding to a change of the flow regime from individual bubbles to a gas jet regime. Knowing τ_{dead} one can calculate the actual life-time of the bubble surface [11]

$$\tau = \nu^{-1} - \tau_{dead}\,. \tag{2.9}$$

Three computer programs are available for determination of $\sigma(t)$ which differ by the approximations made in calculating of the respective quantities. Since these programs give close results for the dynamic surface tension [23], here we discuss only the data computed by the last program. Figure 3 represents data for the dynamic surface tension of one and the same surfactant solution of concentration 3 × CMC obtained by three successive measurements numbered 1, 2 and 3. The increase of the surface tension at each subsequent measurement is due to exhausting of surfactant from the solution of volume 25 ml by the gas bubbles. The same effect, although less pronounced, was observed also at higher surfactant concentrations. That is why we carried out the measurements of a particular solution only once and then replaced the working solution with a new one for the new measurements.

Kinetics of adsorption on expanding interface

In this section we derive analytical expressions for the kinetics of adsorption from micellar surfactant solutions in the case of an expanding interface. It models the adsorption on a gas bubble growing on the tip of a capillary immersed in the surfactant solution. Due to expansion the adsorbed layer stretches and the surface monomer concentration decreases, hence, the surface tension increases. From the other side surfactant molecules (monomers) tend to adsorb onto the bubble surface in order to balance their insufficiency there which leads to lowering of the surface tension. The counteraction of these two tendencies determines the dynamic surface tension of the bubble. The presence of micelles in the solution sufficiently affects the transport of monomers towards the surface by diffusion.

We account for this effect using the equation

$$\frac{\partial \xi_1}{\partial t} - \dot{\alpha}\delta_D \frac{\partial \xi_1}{\partial x} = D_1 \frac{\partial^2 \xi_1}{\partial x^2} - \frac{1}{\tau_M}\xi_1 \tag{3.1}$$

motivated in refs. [3, 4]. Here $\xi_1(x,t) = (c_1 - \bar{c}_1)/\bar{c}_1$ is dimensionless concentration of the monomers, where c_1 is the concentration of free monomers and $\bar{c}_1 = \mathrm{CMC}$ (bar above the letter denotes equilibrium quantity); $\delta_D = d\bar{\Gamma}/d\bar{c}_1$ is the characteristic diffusion length; D_1 is the diffusivity of the monomers; τ_M is the characteristic time of demicellization. The most important boundary condition for solving Eq. (3.1) is the surface balance of monomers

$$\frac{d\Gamma}{dt} + \dot{\alpha}\Gamma = D_1 \bar{c}_1 \left.\frac{\partial \xi_1}{\partial x}\right|_{x=0}, \tag{3.2}$$

where Γ is the adsorption and $\dot{\alpha}$ is the rate of expansion of bubble surface of area $A(t)$

$$\dot{\alpha} = \frac{1}{A}\frac{dA}{dt}.$$

Equation (3.1) is derived assuming that the free monomers and the micelles are of equal diffusivities [4] and that the velocity of liquid flow due to expansion of the bubble surface is $v(x,t) \approx -\dot{\alpha}(t)\delta_D$. The last expression is an oversimplified version of the equation of Van Voorst Vader [24] where we simply replace the x-coordinate by the diffusion length δ_D [3, 25]. Although this approximation was succesfully applied in describing experimental data for the dynamic surface tension [3, 25, 26] it can be of limited validity for particular cases of adsorption. For example, at steady state the time derivatives in Eqs. (3.1) and (3.2) drop out and the integration gives for the subsurface concentration

$$c_1(0,t) = \bar{c}_1 - \frac{2\bar{\Gamma}\,(d\bar{c}_1/d\bar{\Gamma})}{1 + \sqrt{1 + (4D_1\,(d\bar{c}_1/d\bar{\Gamma})/\dot{\alpha}\tau_M)}}.$$

For micellar solutions the last equation predicts dependence of the subsurface concentration on time through the rate of expansion $\dot{\alpha}(t)$. However, it fails for solutions below CMC where the term accounting for the expansion is zero, $(1/\tau_M) \to 0$, and the subsurface concentration remains constant. This is in contrast to the respective equation of Van Voorst Vader and can be explained by the fact that the convective and diffusion terms in Eqs. (3.1) and (3.2) become of one and the same order. Such a problem does not exist if the time derivatives are also kept, which is demonstrated below by numerical computations (see Fig. 4).

Integrating Eqs. (3.1) and (3.2), we assume constant rate of bubble expansion although the bubble surface changes with the time in a complicated way. The expression for $\dot{\alpha}$ is obtained experimentally in [27]. Since the surface tension does not depend essentially on the type of expansion of the bubble surface [25, 27], one can replace the experimental function $A(t)$ by a linear dependence [27]

$$A(t) = A_c\left(1 + \frac{t}{\tau}\right), \tag{3.3}$$

where $A_c = \pi r^2$ is the cross-section area of the capillary and τ is the time for blowing of an air bubble, defined by Eq. (2.9). At the beginning (when $t = 0$) the surface area A is equal to A_c. At $t = \tau$ respectively $A = 2A_c = 2\pi r^2$, which corresponds to hemispherical bubble and maximum bubble pressure. The respective equation for the rate of expansion

$$\dot{\alpha}(t) = \frac{1}{\tau\,(1 + (t/\tau))} \tag{3.4}$$

predicts that $\dot{\alpha}$ decreases with time from $1/\tau$ at the beginning of the process to $0.5/\tau$ at its end. To solve the diffusion Eq. (3.1), we replace (3.4) by its average value [27]

$$\dot{\alpha} = \frac{1}{\tau}\int_0^\tau \dot{\alpha}(t)\,dt = \frac{\ln 2}{\tau}, \tag{3.5}$$

which is already constant throughout the expansion of a single bubble.

The final result for the dynamic surface tension is [3]

$$\begin{aligned}\frac{\Delta\sigma(T)}{\Delta\sigma_0} = {} & \frac{1}{2G}\,e^{-\frac{b^2}{4}T}\left\{(1+G)\mathrm{E}\left[(1+G)\frac{\sqrt{T}}{2}\right]\right. \\ & \left. -(1-G)\mathrm{E}\left[(1-G)\frac{\sqrt{T}}{2}\right]\right\} \\ & +\frac{\varepsilon}{2\Delta\sigma_0}\frac{a}{2a^2-\beta}\left\{3a - b\left\{1 - e^{-\frac{b^2}{4}T}\mathrm{E}\left[b\frac{\sqrt{T}}{2}\right]\right\}\right. \\ & +\frac{1}{2G}\,e^{-\frac{b^2}{4}T}\left\{(1-G-3a)\right. \\ & \times(1+G)\mathrm{E}\left[(1+G)\frac{\sqrt{T}}{2}\right] \\ & \left.\left.-(1+G-3a)(1-G)\,\mathrm{E}\left[(1-G)\frac{\sqrt{T}}{2}\right]\right\}\right\},\end{aligned} \tag{3.6}$$

where $\Delta\sigma = \sigma(t) - \bar{\sigma}$; $\Delta\sigma_0 = \Delta\sigma(0)$; $T = t/\tau_D$ is dimensionless time;

$$\tau_D = \frac{\delta_D^2}{D_1} \tag{3.7}$$

is characteristic time of diffusion; $a = \dot{\alpha}\tau_D$ is dimensionless rate of expansion;

$$\beta = \tau_D/\tau_M \tag{3.8}$$

is dimensionless parameter, which gives the ratio between the time for diffusion of the monomers and the time for their production as a result of the micelle disintegration;

$$b = a^2 + 4\beta$$

is dimensionless parameter; ε is the Gibbs' elasticity defined by

$$\varepsilon = -\bar{\Gamma}\frac{d\bar{\sigma}}{d\bar{\Gamma}}. \tag{3.9}$$

The parameter G is given as

$$G = \sqrt{1 - a(6-a) + 4\beta}, \tag{3.10}$$

and the function E is

$$\mathrm{E}(z) = e^{z^2}[1 - \mathrm{erf}(z)], \tag{3.11}$$

where erf(z) is the error function

$$\mathrm{erf}(z) = \frac{2}{\sqrt{\pi}}\int_0^z e^{y^2}dy. \tag{3.12}$$

Equation (3.6) represents the relaxation of the surfce tension, affected by the convection and the expansion of the bubble surface and also by the destruction of micelles. Due to the made approximations the first two affects are accounted for by the dimensionless parameter a, while the third one - by the dimensionless parameter β. Depending on the magnitudes of a and β there are particular cases of Eq. (3.6) considered below.

At surfactant concentration below CMC (there are no micelles in the solution) $\beta = 0$, because $\tau_M \to \infty$. According to (3.10) $G = \sqrt{1 + a(a-6)}$ and Eq. (3.6) transforms into Eq. (2.18) from ref. [25]. In the particular case of a surface without expansion, it simplifies to the Sutherland's equation [28, 29].

When the surface area does not change with time, $a = 0$, Eq. (3.6) reads [4]

$$\frac{\Delta\sigma(T)}{\Delta\sigma_0} = \frac{1}{2G}e^{-\beta T}\left\{(1+G)\mathrm{E}\left[(1+G)\frac{\sqrt{T}}{2}\right] - (1-G)\mathrm{E}\left[(1-G)\frac{\sqrt{T}}{2}\right]\right\}. \tag{3.13}$$

Therefore, Eq. (3.6) consists of two basic terms. The first term accounts for the relaxation of the surface tension due to increase of the adsorption of surfactant molecules. It decays with the time since for a non-expanding surface it is necessary $\sigma(t) \to \bar{\sigma}$ at $t \to \infty$. The second term, containing the Gibbs' elasticity ε, accounts for the effect of expansion of the bubble surface with the time which effectively decreases the adsorption, i.e., increases the surface tension. The last term will grow with time starting from zero at $t = 0$. The counteraction of these two terms will determine the time dependence of σ. In the maximum bubble pressure experiments $\sigma(t)$ always decreases with time, which means that the first term dominates over the second one. Favoring of the second term was observed experimentally for the interfacial tension of an oil drop expanding at constant rate in surfactant solution [26]. Both two terms contain the effect of the micelles because, by making the surface tension to relax faster, the micelles affect in turn the convective transfer of monomers.

There is a peculiar point at $G = 0$, i.e., at $a(6-a) = 1 + 4\beta$, which leads to special cases depending on the ratio between a and β. Since they were not discussed in [3], we will consider them more thoroughly:

(i) $a(6-a) < 1 + 4\beta$.

In this case the error function is calculated by numerical integration of Eq. (3.12). If $4\beta < a(6-a)$, i.e., $G < 1$, the function E is calculated by (3.11). At $4\beta > a(6-a)$, i.e., $G > 1$, the argument of this function $(1-G)\sqrt{T}/2$ becomes negative, which gives for (3.11)

$$\mathrm{E}(-z) = 2e^{z^2} - e^{z^2}[1 - \mathrm{erf}(z)], \tag{3.14}$$

where $z = (G-1)\sqrt{T}/2$. The numerical procedure for calculating E is described in [25].

(ii) $a(6-a) > 1 + 4\beta$.

Then G becomes complex because of the negative radical quantity. Introducing the imaginary quantity $G^* = iG_0$, where

$$G_0 = \sqrt{a(6-a) - (1+4\beta)}$$

we can write (3.11.) as [25]

$$\mathrm{E}(iz) = U - iV, \qquad z = (1+G)\sqrt{T}/2,$$

$$\mathrm{E}(-iz) = U + iV, \qquad z = (1-G)\sqrt{T}/2.$$

Here z is a complex argument

$$z = G\frac{\sqrt{T}}{2} + i\frac{\sqrt{T}}{2},$$

whereas $U(z)$ and $V(z)$ are the real functions

$$U(\xi,\zeta) = \frac{2}{\sqrt{\pi}}e^{\zeta^2}\int_\xi^\infty e^{-y^2}\cos[2\xi(y-\zeta)]\,dy \tag{3.15a}$$

$$V(\xi,\zeta) = \frac{2}{\sqrt{\pi}}e^{\zeta^2}\int_\xi^\infty e^{-y^2}\sin[2\xi(y-\zeta)]\,dy \tag{3.15b}$$

which can be calculated by numerical integration. In view of the above definitions Eq. (3.6) transforms into:

$$\frac{\Delta\sigma(T)}{\Delta\sigma_0} = e^{-\frac{b^2}{4}T}\left(U - \frac{V}{G_0}\right) + \frac{\varepsilon}{2\Delta\sigma_0}\frac{a}{2a^2-\beta} \times\left\{3a - b\left[1 - e^{-\frac{b^2}{4}T}\mathrm{E}\left(\frac{b}{2}\sqrt{T}\right)\right] - \left[3aU - \frac{V}{G_0}(3a-b^2)\right]e^{-\frac{b^2}{4}T}\right\}. \tag{3.16}$$

Based on the analytical expressions summarized above we calculated the dynamic surface tension at different values of the parameters. The results of such calculations for solutions without micelles ($\beta = 0$) presented in Fig. 4a illustrate the net effect of the bubble expansion. The calculations are performed assuming that the rate of bubble expansion $\dot{\alpha}$ depends on time in the following way:

$$\dot{\alpha}(t) = \frac{\ln 2}{t} \tag{3.17}$$

(cf. Eq. (3.5)). In fact, integrating the diffusion equation (3.1), we assumed that $\dot{\alpha}$ does not depend on time during the formation of one bubble. The introduction of time dependence of $\dot{\alpha}$ in the final equations is suggested by the way the experimental data for $\sigma(t)$ are obtained by the maximum bubble pressure method. In this case, as pointed out in [27], each point from the dependence of σ on t correponds to an individual bubble. This value is not a current value of σ for one and the same surface, as it is for the other methods, e.g. oscillating jet and inclined plate. In this way the variable t runs different values of τ, corresponding to different bubbles of different life-times. This feature of the maximum bubble pressure method can be accounted for by introducing in the final expression for $\sigma(t)$ a quantity $\dot{\alpha}$, depending on the time t, instead of the constant rate of expansion assumed in solving the diffusion problem.

The solid lines in Fig. 4a represent the dynamic surface tension $\sigma(t)$ at different values of the characteristic diffusion time τ_D. It is seen, that with decreasing of τ_D the surface tension decreases more rapidly. Since in this case the diffusion of monomers proceeds faster, it compensates more successfully the increase of the surface tension due to bubble surface expansion. The dashed line corresponds to the case of non-expanding surface at the smallest diffusion time (0.1 s). In this case the surface tension decreases faster in comparison to the expanding surface, which implies the importance of the bubble area expansion.

Figure 4b illustrates the effect of the micelles on the dynamic surface tension at different values of the parameter β. All curves are drawn by Eq. (3.6) at one and the same diffusion time $\tau_D = 1$ s. When β increases, i.e., the micellization time τ_M decreases compared to the diffusion time τ_D, the surface tension decreases faster. This fact can be explained with the contribution of micelles to the diffusion owing to the influx of monomers, released by the micelles.

Fig. 4 Effect of the bubble area expansion on the dynamic surface tension: a) Model system below CMC. The solid lines are computed at different values of the diffusion time τ_D assuming expansion rate $\dot{\alpha}(t)$ defined by Eq. (3.17). The dashed line is at constant bubble area; b) Model system above CMC. The lines are computed at different values of the parameter β and at expansion rate (3.17)

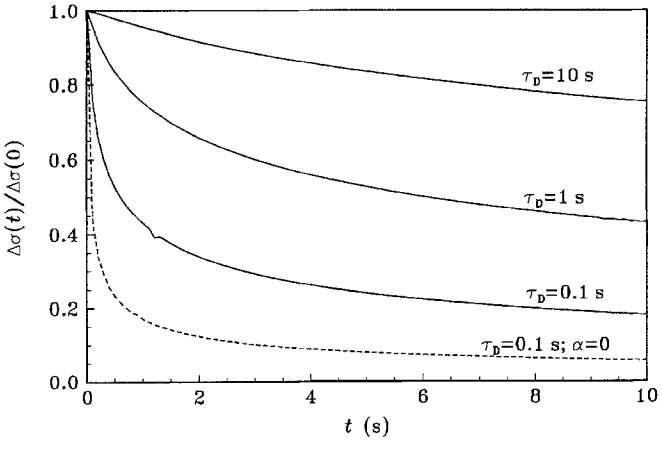

(a)

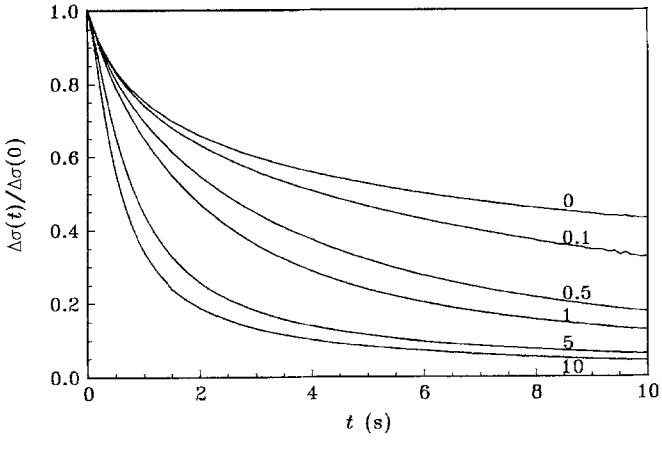

(b)

Results

Oscillating jet method

The experimental data for $\sigma(t)$ in Fig. 5 show that the surface tension measured by three different capillaries decreases with time tending to the equilibrium value $\bar{\sigma}$. With increasing of the surfactant concentration the surface tension decreases more quickly, because the micelles accelerate the adsorption kinetics by supplying the surface layer with monomers. Similar trends are observed also in the experiments performed by the inclined plate and the maximum bubble pressure method (see below). Since the jet surface does not expand during the experiments the data are processed by Eq. (3.14) at two adjustable parameters: characteristic time of diffusion τ_D and characteristic time of demicellization τ_M. As seen from the figures the theory describes fairly well the experiment except for capillary

Fig. 5 Surface tension of micellar solutions of Triton X-100 measured by different capillaries of the oscillating jet: a) capillary 1 ($r_1 = 0.0342$ cm); b) capillary 2 ($r_2 = 0.0288$ cm); c) capillary 3 ($r_3 = 0.0218$ cm). The concentrations shown in the legend are in times CMC. The solid lines are theoretical fits of the data

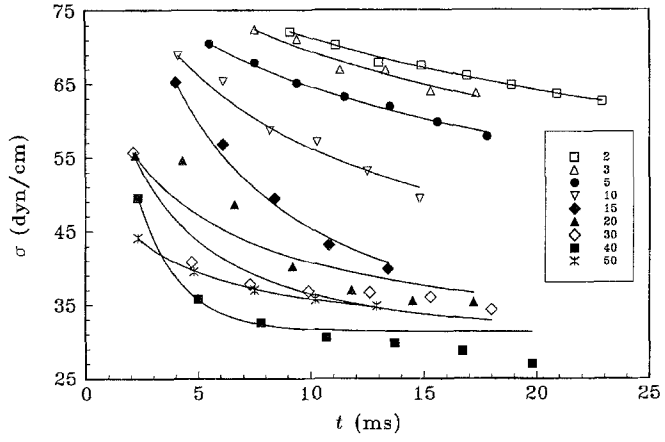

(a)

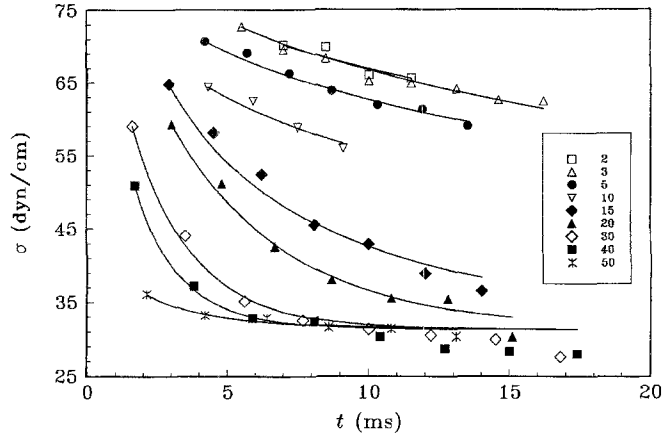

(b)

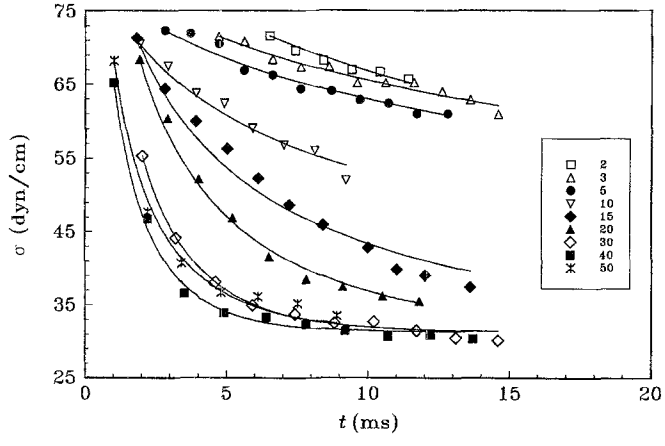

(c)

3 at the lowest surfactant concentrations. This can be due to exhausting of surfactant molecules from the solution by foaming. The values of τ_D and τ_M obtained by the numerical fits are plotted in Fig. 6.

The characteristic time of diffusion τ_D was found to decrease above CMC (Fig. 6a) which means increasing of the contribution of the free monomers to the diffusion. As defined by Eq. (3.7), this time should remain constant above CMC because the derivative $d\bar{\Gamma}/d\bar{c}_1 = \delta_D$ is taken at CMC. This corresponds to the fact that above CMC the number of free monomers remains constant at equilibrium conditions. Maintaining constant τ_D, as done for sodium dodecylsulfate solutions [3], did not give good fits of the data for Triton X-100. For this reason we are using τ_D as a second adjustable parameter.

The characteristic time of demicellization τ_M tends to decrease, implying an increased contribution of the micelles to the surfactant adsorption (Fig. 6b).

Fig. 6 Time constants calculated theoretically from the experimental data in Fig. 5 measured by the oscillating jet: a) characteristic time of diffusion; b) characteristic time of micellization

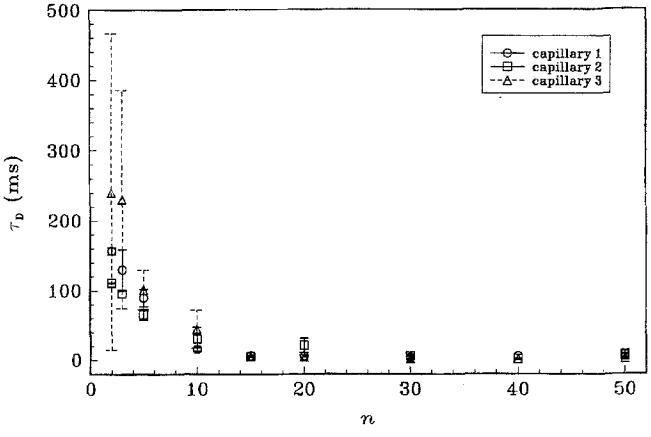

(a)

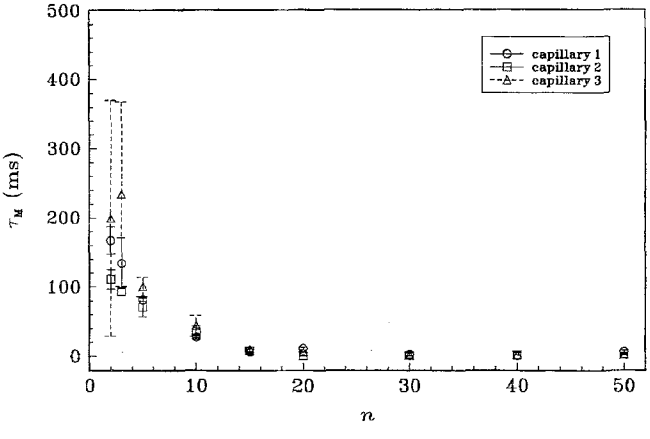

(b)

The points for τ_D and τ_M are mean values calculated for two different measurements of the surface tension by one and the same capillary. The error bars represent the deviation of the two values from the mean. The deviation is larger at relatively small surfactant concentrations close to CMC which can be explained with poorer reproducibility of the surface tension relaxation due to less developed micellar system. With increasing of the surfactant concentration this deviation decreases. The largest deviation is found with capillary 3 which is of the smallest radius.

Inclined plate method

This method is suitable only at low concentrations of Triton X-100 (until $5 \times$ CMC) where the surface tension relaxation is relatively slow. The experimental results shown in Fig. 7 are part of the data from Fig. 3 processed by Eq. (3.14) at constant surface area. The values of τ_D and τ_M are of comparable magnitude which differ appreciably from the respective values obtained by the other two experimental methods. For example, the characteristic time of diffusion τ_D is between 800 and 1080 ms whereas the characteristic time of demicellization τ_M is about 1000 and 1390 ms. This difference can be attributed to the time scale of the experimental method which affects the numerical procedure.

Maximum bubble pressure method

The experimental results shown in Fig. 8 are processed by Eqs. (3.6) and (3.16). As one can expect, the calculated values of τ_D are comparable with these, obtained by the oscillating jet method because both methods are operating

Fig. 7 Surface tension of micellar solutions of Triton X-100 measured by the inclined plate. The concentrations shown in the legend are in times CMC. The solid lines are theoretical fits of the data

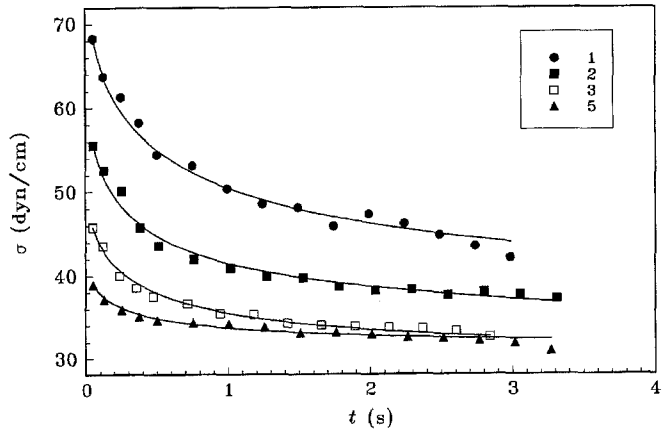

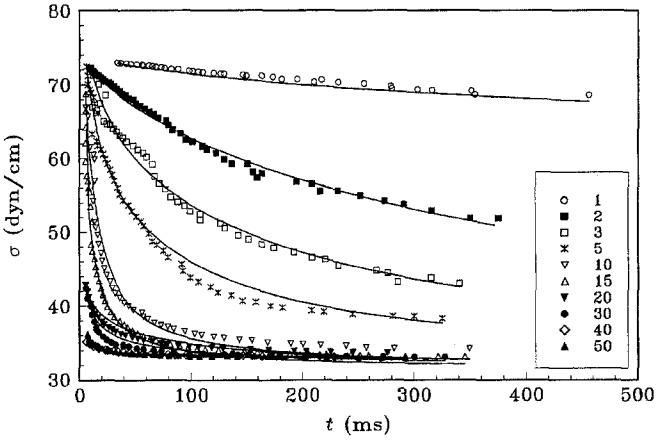

Fig. 8 Dynamic surface tension of micellar Triton X-100 measured by the maximum bubble pressure method. The concentrations shown in the legend are in times CMC. The solid lines are theoretical fits of the data accounting for the bubble area expansion

at commensurable time scales. The characteristic time of diffusion τ_D decreases with increasing of the concentration due to increased contribution of the free monomers (Fig. 9a). The characteristic time of micellization τ_M also decreases with increasing of the concentration till $20 \times$ CMC, where τ_M reaches a minimum value. Above this concentration τ_M sharply increases to reach values from 0.5 to 0.8 s, while τ_M measured by the oscillating jet increases insignificantly. The difference in τ_M measured by the two methods is discussed in the next section.

There is one more parameter of the data fits – the Gibbs' elasticity ε plotted in Fig. 9b – which results from the expansion of the bubble surface. Although the Gibbs' elasticity does not exhibit a pronounced concentration dependence it seems that it passes through a minimum at $20 \times$ CMC. The values of ε are of right order of magnitude which can be proven by means of the equation [29]

$$\varepsilon \sqrt{\tau_D} = \frac{R_g T_a \bar{\Gamma}^2}{\bar{c}_1 \sqrt{D_1}}, \tag{4.1}$$

where $R_g = 8.314 \times 10^7$ erg/mol·K is the universal gas constant, $T_a = 297$ K is the absolute temperature. The monomer diffusivity of Triton X-100 is 10^{-6} cm^2/s [8]. At $\tau_D \sim 10^{-2}$ s and $\varepsilon \sim 100$ dyn/cm we calculated an equilibrium adsorption $\bar{\Gamma} \sim 2.5 \times 10^{-10}$ mol/cm^2 in accord with literature data $\bar{\Gamma} = 3 \times 10^{-10}$ mol/cm^2 [8].

Discussion

We have discussed the main experimental and theoretical results obtained by our investigation of the kinetics of surface tension of micellar Triton X-100 solutions. They

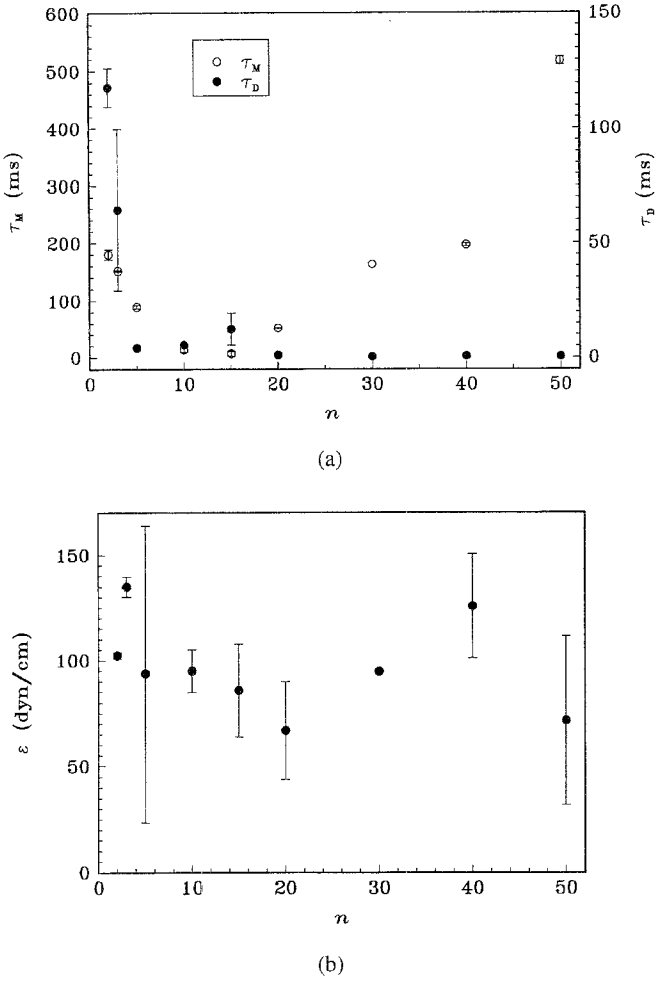

Fig. 9 Parameters of the fit calculated theoretically from the experimental data in Fig. 8 measured by the maximum bubble pressure: a) characteristic time of diffusion τ_D and characteristic time of micellization τ_M; b) Gibb's elasticity ε. Error bars represent the deviation from the mean of two successive measurements

are a continuation of our previous studies on the same surfactant [2, 8, 10] which showed that it is a suitable model system for illustration of the effect of the micelles on the surface tension relaxation at wide concentration range. Here we apply simultaneously three experimental methods in order to receive reliable experimental data. In contrast to the approximate theories previously used to account for the micellization kinetics we utilize in this study a rigorous theoretical model adequately describing the particular experiments.

Comparison of the experimental methods

The chemical relaxation techniques [5–7] detect directly the variation of the surfactant concentration in the bulk of solution which decays exponentially with time if small perturbations from equilibrium are applied. Depending on the way of perturbation, these methods can give appreciably different values for the demicellization time constants for one and the same system [3]. The surface relaxation methods, although easier to perform, are less direct tools for studying the micellization kinetics, because the subsurface concentration depends also on the transportation of surfactant species by diffusion and, hence, on the way the surface adsorption layer is perturbed.

The usage of three experimental methods working at different time scales allowed to obtain a more comprehensive picture of the micellization kinetics. The experimental data should be as reliable as closer the time scales of the experimental method and that of the micellization process are. It is quite possible to obtain unlike values of the surface tension measured by the different methods in one and the same time interval. The reason is that the kinetics of the surface tension, being a non-equilibrium process, depends on characteristics of the particular experiment which cannot always be kept uniform, i.e., disturbance of the surface, e.g., rate of expansion of the air bubble surface [27], registration and calculation of the surface tension.

Nevertheless, a good coincidence of the data from different methods was obtained, especially at intermediate surfactant concentrations, shown in Fig. 10 for 15 × CMC. The experimental points for the oscillating jet at very small times (up to several milliseconds) overlap with the points for the maximum bubble pressure at times about several hundred milliseconds, which then pass into the data for the inclined plate of the order of several seconds. The lack of good coincidence of the data measured by the three methods at smaller concentrations can be explained with the insufficient number of micelles in the bulk which makes them more sensitive to the way of perturbation.

Fig. 10 Comparison of the surface tension measured as a function of time by three experimental methods. The surfactant concentration is 15 × CMC

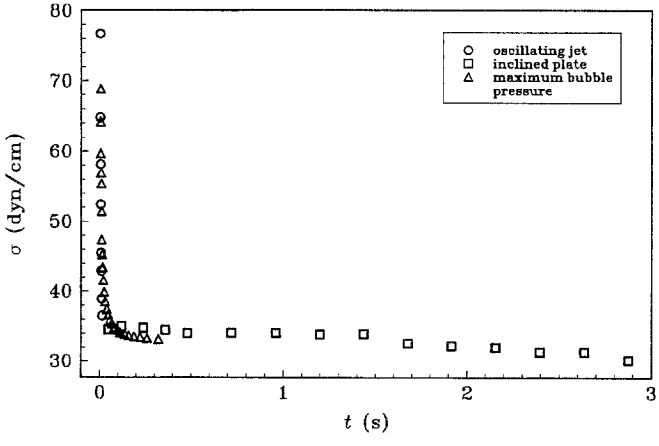

For the inclined plate the values of τ_D and τ_M differ appreciably from the respective values obtained by the other two experimental methods (oscillating jet and maximum bubble pressure). The inclined plate detects the long time asymptotics of the surface tension, while the oscillating jet gives the surface tension at very short times. This reflects the numerical fit of the data because we used the first experimental value of the surface tension, instead of the initial surface tension σ_0 (at $t \to 0$) which is unknown experimentally. This overestimated the contribution of the long times for the inclined plate, where there are missing data for the high initial jump in the surface tension at small times. Such a jump can be detected only by the other two methods which ought to consider them as more realistic. From the other side, the kinetics of the surface tension at long or short times can in principal be determined by different micellization processes. For example, the slow process of micellization can prevail in the inclined plate experiments, while the fast process can do so in the oscillating jet and maximum bubble pressure experiments. However, it turned out that τ_M, determined by the oscillating jet and the maximum bubble pressure corresponds in fact to the characteristic time of the slow process of micellization τ_S, measured by bulk relaxation techniques (see the next subsection). At the same time the respective time of the fast process τ_F is orders of magnitude less than τ_S [12]. Therefore, the time constants measured by the inclined plate may not correspond to a real process of micellization. Their larger values can be due to an artefact of the numerical fit of the data or to hydrodynamic flow in the plate canal and expansion of the adsorption layer not accounted for by the theory.

Characteristic times of micellization

Here we compare the numerical results for the time constant of micellizaiton τ_M, obtained by us, with literature data for the same surfactant (Triton X-100). In Fig. 11 is plotted the reverse micellization time $1/\tau_M$ versus the relative amount of surfactant aggregated in micelles

$$\theta = \frac{\bar{c} - \mathrm{CMC}}{\mathrm{CMC}} = n - 1 ,$$

where $\bar{c}$ is the total Triton X-100 concentration. This plot of the data is suitable for their interpretation, based on the theory of Aniansson and Wall [5–7] for the kinetics of micellization in bulk surfactant solutions. These authors have derived expressions for the characteristic times of fast and slow relaxation, τ_F and τ_S. The fast relaxation process is attributed to the release of several monomers by a micelle, which makes the micelle less stable. The slow

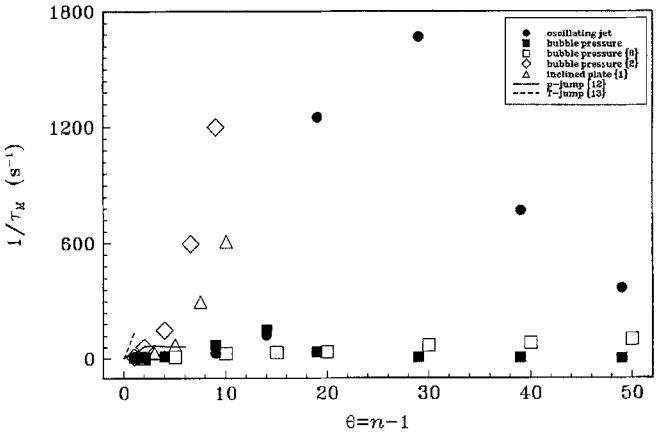

Fig. 11 Reverse micellization time plotted versus the relative amount of Triton X-100 aggregated in the micelles. The solid figures are our experimental data from Figs. 6 and 9a obtained by surface tension experiments. The empty figures represent literature data from such experiments. The lines are data obtained by bulk relaxation experiments (p-jump and T-jump) at 20 °C [12] and 10 °C [13]

process is due to gradual disappearance of the micelles. Each one of these processes is described by a typical dependence of the respective time constant on θ. While the reverse time constant of fast relaxation $\tau_F^{-1}(\theta)$ increases linearly with θ, the reverse time of the slow process $\tau_S^{-1}(\theta)$ depends in complicated way on θ passing through a maximum and/or minimum. The respective expressions for the time constants are derived assuming small deviations from equilibrium, attained by the bulk relaxation techniques. The theory [5–7] is valid strictly only at surfactant concentrations near CMC.

First, we discuss our data for the characteristic micellization time τ_M plotted by solid figures. One can see from Fig. 11 that at low concentrations ($\theta < 15$) the time constants τ_M, obtained by two independent methods (oscillating jet and maximum bubble pressure) are of one and the same order. With increasing of the concentration $1/\tau_M$ also increases in accordance with the literature data obtained by bulk relaxation methods: p-jump [12, 13] and T-jump [13]. Since at higher concentrations such data are missing in literature, one can only guess the magnitude of $1/\tau_M(\theta)$, extrapolating the known values to large θ. They are enough, however, to conclude that our τ_M corresponds to the slow relaxation process of micellization because the time constant of the fast process is several orders of magnitude smaller [12].

At higher concentrations the two methods give appreciably different values for τ_M which can be explained by incompatibility of the methods when very fast relaxation of the surface tension is studied. A transition from single bubbles to formation of couples of bubbles (bubble jets) can occur at very high bubbling frequencies [27]. This

can change in turn the rate of surface expansion, i.e., the way of creation of initially clean surface. In the oscillating jet this is a result of continuous refreshing of the surface leading to different initial adsorption of surfactant and different initial rate of surface expansion.

The second reason for the observed difference in the values of τ_M can be the procedure of processing the experimental data. The surface of the air bubble expands with different rates, while the surface adsorption layer of the jet does not change its area. The rate of bubble expansion is accepted to be constant in our theoretical model, because the evolution of the bubbles has not been recorded as in ref. [27]. This introduces a new parameter of the model, the Gibbs' elasticity ε, which although realistic (see previous section) can lead to increase of τ_M in the data fit (decrease of $1/\tau_M$) compared to the oscillating jet. Another problem can be a different degree of deviation of the subsurface concentrations of the monomers and micelles from the equilibrium ones, important for the applicability of the theoretical models derived at small perturbations. This deviation seems rather large in the oscillating jet where, looking at unrealistically high initial values of the surface pressure, a completely clean surface should be reached at very small times. In the maximum bubble pressure there is a residual adsorption layer remaining after the previous bubble is blown which effectively decreases the initial surface tension [27]. This difference can lead to smaller time constants τ_M measured by the oscillating jet.

We compare in Fig. 11 our data for the micellization time τ_M also with literature data obtained by surface relaxation methods (open symbols). It is seen that our data measured by the maximum bubble pressure are in good agreement with the data of Geeraerts and Joos [8] obtained by the same method. Our values for the oscillating jet are of the same order as the values measured by inclined plate [1] and by maximum bubble pressure [2]. They were obtained, however, by fitting the experimental data with approximate models favoring only the initial stages of relaxation.

References

1. Rillaerts E, Joos P (1982) J Phys Chem 86:3471
2. Makievski AV, Fainerman VB, Joos P (1994) J Colloid Interface Sci 166:6
3. Dushkin CD, Iliev TzH, Radkov YS (1994) Colloid Polym Sci 273:370
4. Dushkin CD, Ivanov IB, Kralchevsky PA (1991) Colloids Surfaces 60:235
5. Aniansson EAG, Wall SN (1974) J Phys Chem 78:1024
6. Aniansson EAG, Wall SN (1975) J Phys Chem 79:857
7. Aniansson EAG, Wall SN, Almgren M, Hoffmann I, Ulbricht W, Zana R, Lang J, Tondre C (1976) J Phys Chem 80:905
8. Geeraerts G, Joos P (1994) Colloids Surfaces 90:149
9. Fainerman VB, Rakita YuM (1990) Kolloidn Zh 52:106 (in Russian)
10. Fainerman VB, Makievski AV, Joos P (1994) Colloids Surfaces 90:213
11. Fainerman VB, Miller R, Joos P (1994) Colloid Polym Sci 272:731
12. Chan S-K, Herrmann U, Ostner W, Kahlweit M (1977) Ber Bunsenges Phys Chem 81:396
13. Herrmann U, Kahlweit M (1980) J Phys Chem 84:1536
14. Defay R, Petre G (1971) Surf Colloid Sci 3:27
15. Defay R, Petre G (1971) In: Surface and Colloid Science, Matijevic E (ed), Wiley Interscience, New York
16. Bohr N (1909) Phil Trans Roy Soc (London) A 209:281
17. Hansen RS (1964) J Phys Chem 68:2012
18. Lord Rayleigh (1890) Proc Roy Soc (London) 47:281
19. Petre G (1970) Thesis Brussels
20. Van den Bogaert R, Joos P (1979) J Phys Chem 83:2244
21. Posner AM, Alexander AE (1949) Trans Faraday Soc 45:651
22. Davies JT, Makepeace RW (1978) AIChE J 24:524
23. Mitrancheva JV (1994) TEMPUS Thesis, University of Sofia (in Bulgarian)
24. Van Voorst Vader F, Erkens ThF, Van den Tempel M (1964) Trans Faraday Soc 60:1
25. Dushkin CD, Iliev TzH (1994) Colloid Polymer Sci 272:1157
26. Horozov T, Dushkin C (1993) In: Proceedings of the World Congress on Emulsions, Paris, 2:32–136
27. Horozov TS, Dushkin CD, Danov KD, Arnaudov LN, Velev OD, Basheva ES, Ivanov IB, Mehretab A, Broze G (1995) Colloids Surfaces (in press)
28. Sutherland KL (1952) Austral J Sci Res A5:683
29. Joos P, Van Hunsel J (1988) Colloids Surfaces 33:99